TIGHTENING BILINEAR RELAXATIONS WITH 45° ROTATIONS*

JAIVARDHAN SOOD† AND JAY M. ROSENBERGER‡

Abstract.
A classical approach for handling non-convex optimization problems involving bilinear terms is to approximate the bilinear expressions using McCormick relaxations. Such relaxations are central to global optimization methods, with the spatial branch-and-bound (sBB) algorithm being one of the most widely used approaches. In the spatial branching step, the algorithm partitions the feasible region using axis-aligned (parallel-axis) cuts, generating hyper-rectangular sub-region. In this research, we investigate the impact of introducing 45°-oblique cuts instead of traditional axis-aligned cuts. We show that oblique cuts can provide improved directional bounds—either upper or lower—depending on the orientation of the cut. More precisely, we demonstrate that the upper (respectively, lower) bounds derived from the proposed oblique-envelope formulation are always tighter than the corresponding McCormick upper (respectively, lower) bounds over the associated feasible region. Furthermore, we derive conditions under which the range of the true bilinear function over the feasible region induced by axis-aligned cuts exceeds the corresponding range over the feasible region induced by oblique cuts. These results provide theoretical justification for the potential tightening effect of oblique partitioning in spatial branch-and-bound algorithms.

Key words. Non-Convex Optimization, Bilinear Terms, Convex and Concave Envelopes

MSC codes. 15A06, 90C26, 90C90

1. Introduction and Motivations.

Bilinear terms, defined as two decision variables multiplied with each other, are one of the most commonly occurring non-convex expressions in optimization problems. Mathematically, a bilinear function can be defined as $f(x, y) = x \cdot y$, where x and y are decision variables for an optimization problem.

They occur in real-world applications such as pooling and blending problems [1, 5, 12, 15], energy systems modeling [11, 14], portfolio optimization [20], and chemical engineering [16, 17, 25]. In the domain of surrogate optimization, which is the main application based motivation behind this research, bilinear terms frequently arise in surrogate model formulations when capturing interactions between variables. Optimizing surrogate models that contain bilinear terms is a challenging and non-trivial task, as such terms introduce non-convexity into the problem as illustrated in Fig 1. The figure illustrates the surface of the bilinear function. It can be observed, the bilinear term is non-convex and exhibits a saddle-shaped geometry, which makes it challenging to optimize globally. A substantial body of literature has been devoted to the optimization of bilinear functions and the development of relaxation techniques.

One of the most commonly used techniques for convexifying bilinear terms is the use of McCormick envelopes. Many modern global optimization solvers, such as COUENNE, MINOTAUR, and BARON, incorporate McCormick relaxations within a spatial Branch-and-Bound (sBB) framework [7, 26]. In sBB, each bilinear or otherwise non-convex term is replaced by its convex relaxation, and the resulting relaxation is solved at the root node to obtain a global lower bound for the optimization problem.

*Submitted to the editors on November 3, 2026.

Funding: The authors are grateful to the National Science Foundation (NSF-CHE-2108767) and Center for Stochastic Modeling, Optimization and Statistics (COSMOS) for partially funding the research study.

†Department of Industrial, Manufacturing, and Systems Engineering, The University of Texas at Arlington, TX - 76013 (jaivardhan.sood@uta.edu).

‡Department of Industrial, Manufacturing, and Systems Engineering, The University of Texas at Arlington, TX - 76013 (jrosenbe@uta.edu,).

This manuscript is for review purposes only.

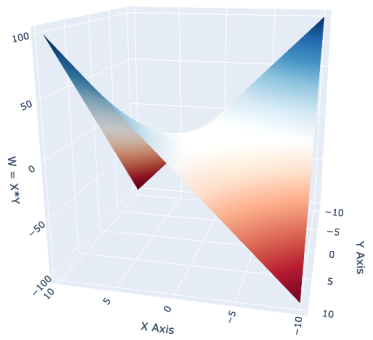


Fig. 1: Surface Plot for Bilinear terms

As branching proceeds, the domains of the variables are further partitioned, and new McCormick relaxations are constructed over the resulting sub-regions. This process is intended to tighten the relaxations, improve bound quality, and accelerate convergence to a global solution. In standard sBB, these sub-regions are generated using axis-aligned cuts. Since tighter relaxations generally lead to stronger bounds and faster convergence, in this work we investigate an alternative approach based on 45° oblique cuts instead of parallel-axis cuts, and compare the performance of the derived bounds with the standard McCormick relaxations.

To describe the McCormick relaxation, consider a bilinear term $z = x \cdot y$ with

$$x \in [x_L, x_U], \qquad y \in [y_L, y_U].$$

The McCormick envelopes replace the non-convex bilinear equality by four linear inequalities: two convex under-estimators and two concave over-estimators. These are given by

$$z \geq x_L y + x y_L - x_L y_L, \tag{1.1}$$

$$z \geq x_U y + x y_U - x_U y_U, \tag{1.2}$$

$$z \leq x_U y + x y_L - x_U y_L, \tag{1.3}$$

$$z \leq x_L y + x y_U - x_L y_U. \tag{1.4}$$

Together, these inequalities define the convex hull of the bilinear term over a rectangle in the two-variable case, and form the basis for many relaxation-based global optimization methods.

The outline of the remainder of this paper is as follows. Section 2 describes related literature, the research gap, and the contribution of this research. Section 3 derives the proposed quadratic under- and over-estimators and establishes the worst-case relaxation-gap results. Section 4 derives the global extrema of the bilinear function over the rotated region. Section 5 compares the exact bilinear ranges over the original and rotated regions and derives the corresponding comparison conditions. Section 6 concludes the paper and discusses directions for future work

2. Literature Review. One of the earliest contributions to addressing bilinear terms in optimization was by McCormick [22], who introduced convex under-

estimators and concave over-estimators for non-convex terms, thereby constructing tight linear relaxations known as McCormick envelopes. This approach enabled approximation of bilinear terms, making them tractable for linear solvers. In the case of a bilinear term, the relaxation is represented by four linear inequalities: two forming the convex under-estimators and two forming the concave over-estimators, as illustrated in Fig 2. McCormick envelopes remain one of the most widely used technique for handling bilinear terms in optimization. One of the key advantages of using McCormick envelopes to handle bilinear terms is that the resulting relaxations remain in the same variable space as the original problem [34].

In contrast, an alternative approach known as the auxiliary variable method (AVM) introduces an additional variable for each bilinear or higher-order term involved in the formulation [31, 32, 33]. Al-khayyal et al. [4] showed that the convex hull for bilinear functions is captured by the McCormick envelopes. Scott et al. [28] generalized the McCormick relaxation framework to extend its applicability beyond simple bilinear terms. Their generalized formulation established key theoretical properties that enabled a rigorous study of McCormick relaxations over subintervals encountered during the branch-and-bound process. As a result, they provided stronger convergence guarantees.

Tsoukalas et al. [34] developed a generalization of the McCormick composition theorem to construct relaxations for multivariate outer functions, extending the original McCormick framework that was limited to univariate outer functions. They derive tighter relaxations for multivariate outer functions. Another notable contribution in the optimization of bilinear terms was made by Ryoo and Sahinidis [25], who proposed reducing the domain of variables prior to branching and, in doing so, established the foundation for the branch-and-reduce algorithm framework.

The αBB algorithm [2, 3] is a well-established relaxation approach for handling smooth nonconvex functions. It is embedded within a branch-and-bound framework and introduces a set of parameters, α_i, that capture the curvature of the non-convex function to generate a tighter convex underestimator. This convexification step provides tighter lower bounds for the global optimization process, while upper bounds are obtained by performing local searches on the original nonlinear formulation.

Another cornerstone contribution to the convexification and linearization of bilinear terms was proposed by Sherali et al. [29], who introduced the Reformulation–Linearization Technique (RLT). As the name suggests, the method consists of two main components - reformulation and linearization. In the reformulation phase, additional nonlinear constraints are generated by multiplying problem constraints with variable bounds. In the linearization phase, these nonlinear terms are replaced with newly introduced variables, resulting in a tractable linear relaxation. Compared to convex envelope methods, RLT is often capable of producing significantly tighter lower bounds, which makes it a powerful approach for handling bilinear optimization problems. However, RLT methods lead to a large number of variables and constraints and may be computationally disadvantageous.

For multilinear terms, McCormick envelopes can be applied recursively. However, such recursive relaxations often yield weak approximations, leading to poor bounds. Luedtke et al. [21] investigated the trade-off between using recursive McCormick relaxations and convex hull characterizations. They showed that recursive McCormick relaxations coincide with the convex hull when the variable bounds are symmetric around zero. Furthermore, they proved that the gap between the concave and convex bounding functions obtained from McCormick relaxations is always within a constant factor of the gap defined by the true convex and concave envelopes. Rikun [24], in

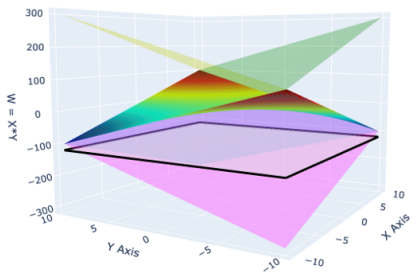


Fig. 2: 3-D plot of McCormick Envelopes for Bilinear terms

their research, derived sufficient conditions to check the polyhedrality of convex envelopes and derived analytical formulas to find some elements of the convex envelopes for general multilinear terms.

Bestuzheva et al. [8], developed an algorithm for efficient separation of RLTcuts to improve the relaxations for bilinear terms. The RLT cuts developed by Sherali et al. [29] introduce excessive cuts making them computationally challenging. In the presence of linear constraints, the McCormick relaxations can be improved upon by adding the RLT cuts. He et al. [18] introduced a two-step approach to find factorable relaxations for composite functions ($f_1(x)f_2(x)$) using outer-approximations. They utilize a two-step procedure that leverages the underestimator on the function $f_i(x)$ and finds linear inequalities, other than the McCormick inequalities, that might tighten the relaxations for composite functions. The relaxations proposed by He et al. [18] are formulated in higher-dimensional space. Wilhelm et al. [35], extended this work by finding improved relaxations for bilinear terms by exploiting information on *a priori* underestimators and overestimators. Importantly, the relaxations proposed by Wilhelm et al. [35] remain within the reduced-space or original problem space.

In a more recent study, Schweidtmann et al. [27] proposed a reduced-size (RS) formulation for the global optimization of Gaussian process (GP) models. They derived new convex underestimators for commonly used covariance functions in GPs, which led to substantially tighter lower bounds compared to those obtained using the complete formulation. This improved the computational efficiency of deterministic global optimization algorithms involving GP-based surrogates.

Semi-definite programming and relaxations are also commonly used in solving non-convex optimization problems [9, 13, 19]. For a broader survey on non-convex mixed-integer non-linear programming, please refer to the review articles by Burer et al. [10] and Belotti et al. [6].

2.1. Motivation and Research Gap. Many global optimization solvers employ the spatial Branch-and-Bound (sBB) algorithm to solve non-convex optimization problems containing bilinear terms, typically relying on relaxations such as the McCormick envelopes [7, 30, 23, 26]. For bilinear terms, the feasible region is represented as a hyper-rectangle defined by bounds on the variables (Fig 3). The sBB algorithm recursively partitions this feasible region (i.e., spatially branches) and con-

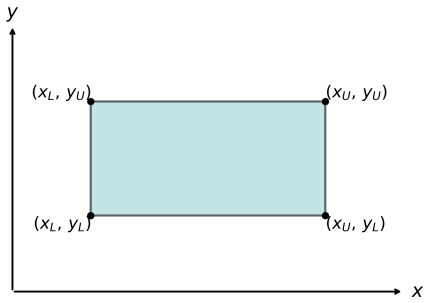
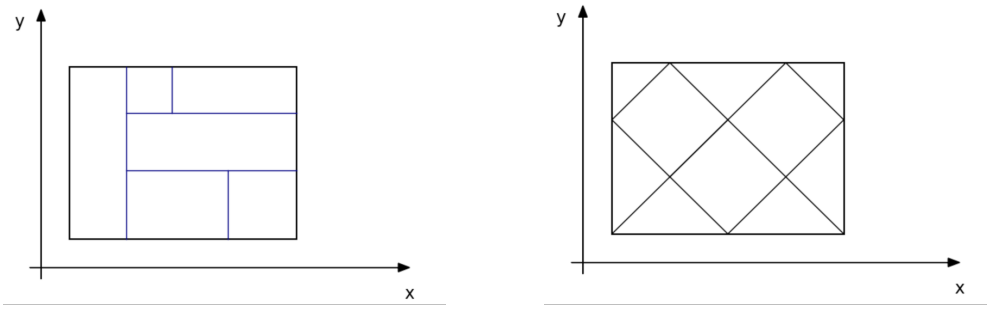


Fig. 3: Feasible Region for Bilinear terms

structs relaxations for each resulting sub-region, thereby tightening the relaxation as the algorithm progresses. The quality of these relaxations plays a crucial role in the performance of the algorithm: tighter relaxations lead to better bounds and improved convergence to the global optimum.



(a) Axis-aligned cuts (b) Oblique cuts

Fig. 4: Spatial Branching Process

As illustrated in Figure 4, the branching step in sBB typically introduces axis-aligned (parallel-axis) cuts, which generate hyper-rectangular sub-regions. In this research, we investigate whether the relaxations for bilinear terms can be improved by introducing 45°-oblique cuts instead of traditional axis-aligned cuts during the branching step. Such oblique cuts produce sub-regions with a diamond-like geometry rather than the standard hyper-rectangular structure.

In this research, we derive bounds for bilinear terms that share this diamond-shaped geometry and compare them with the standard McCormick bounds. Although the present study does not incorporate oblique cuts directly into the branching procedure of the sBB algorithm, we show that tighter directional bounds (either upper or lower) can be obtained compared to the corresponding McCormick bounds. This result provides an initial step toward developing branching strategies based on oblique partitioning for improving relaxations in sBB algorithms.

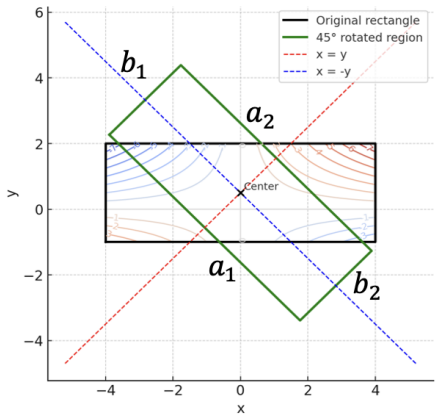


Fig. 5: Rotated feasible sub-region

3. Derivation of Bounds & Main Results.

3.1. Preliminaries & Notation. A bilinear function can be defined as $f(x, y) = x \cdot y$. Let the variable x lie in the interval $x \in [x_L, x_U]$, where x_L and x_U denote the lower and upper bounds of x, respectively. Similarly, the variable y lies in the interval $y \in [y_L, y_U]$, where y_L and y_U denote the lower and upper bounds of y. The feasible region for the bilinear function is illustrated in Figure 3.

To represent the bilinear term within an optimization framework, we introduce an auxiliary variable z such that $z = xy$. The feasible set associated with the bilinear term can therefore be written as

$$R = \{(x, y, z) \in [x_L, x_U] \times [y_L, y_U] \times \mathbb{R} \mid z = xy\}. \tag{3.1}$$

In this section, we derive the bounds for the feasible regions for bilinear terms which have a diamond-like geometrical shape and arise if we were to introduce 45°-oblique cuts instead of parallel axis cuts and also provide our main results for the derived bounds.

3.2. Geometry of Feasible Region for Bilinear Terms. To study the geometry of the feasible sub-regions induced by oblique cuts, we first consider the feasible region associated with a bilinear term. Without loss of generality, assume that the bounds satisfy $x_U - x_L > y_U - y_L$, i.e., the range of the variable x exceeds that of y. Under this condition, the feasible region in the (x, y)-space is a hyper-rectangle that is elongated along the x-dimension. To study feasible sub-regions with a diamond-like geometry, we consider a rotation of the original rectangular feasible region about its center by an angle of 45° in the clockwise direction.

This transformation produces a rotated region whose projection in the original coordinate system exhibits a diamond-like shape, as illustrated in Fig 5. The choice of a 45° rotation is particularly convenient because it yields simple bounds in the sum and difference coordinates. Specifically, $x' + y'$ depends only on $y - k$, while $x' - y'$ depends only on $x - h$. This structure is also consistent with the identity $4x'y' = (x' + y')^2 - (x' - y')^2$, which is exploited in the subsequent analysis.

The resulting rotated coordinate system provides a convenient representation of the bilinear geometry. This rotation is given by

$$\begin{bmatrix} x' \\ y' \end{bmatrix} = \begin{bmatrix} h \\ k \end{bmatrix} + \begin{bmatrix} \cos\theta & \sin\theta \\ -\sin\theta & \cos\theta \end{bmatrix} \begin{bmatrix} x-h \\ y-k \end{bmatrix},$$

where, $h = \frac{x_L+x_U}{2}$ and $k = \frac{y_L+y_U}{2}$, defining the center of the original sub-region.

Substituting $\theta = \frac{\pi}{4}$, where $\cos\frac{\pi}{4} = \sin\frac{\pi}{4} = \frac{1}{\sqrt{2}}$:

$$x' = h + \frac{(x-h)+(y-k)}{\sqrt{2}} \tag{3.2}$$

$$y' = k + \frac{-(x-h)+(y-k)}{\sqrt{2}} \tag{3.3}$$

From equations (3.2) & (3.3), we can derive,

$$x' + y' = h + k + \sqrt{2}(y-k) \tag{3.4}$$

From equation (3.4), we can see that the maximum for $x'+y'$ will be when $y = y_U$. Substituting:

$$y_U = k + y_{\text{hr}}$$

where, $y_{\text{hr}} = \frac{y_U-y_L}{2}$

$$x' + y' \leq \frac{2}{\sqrt{2}}(y_U - k) = \frac{y_U - y_L}{\sqrt{2}}$$

Similarly, the lower bound or minimum for $x' + y'$ will be at y_L. Substituting $y_L = k - y_{\text{hr}}$:

$$x' + y' \geq -\frac{y_U - y_L}{\sqrt{2}}$$

Thus:

$$-\frac{1}{\sqrt{2}}(y_U - y_L) \leq x' + y' \leq \frac{1}{\sqrt{2}}(y_U - y_L)$$

Similarly, we can derive bounds for $x' - y'$. Using equations (3.2) & (3.3), we can derive,

$$x' - y' = h - k + \sqrt{2}(x-h) \tag{3.5}$$

From equation (3.5), we can observe that the maximum for $x' - y'$ occurs at x_U:

$$x' - y' \leq \frac{x_U - x_L}{\sqrt{2}}$$

Similarly, the minimum occurs at x_L:

$$x' - y' \geq -\frac{x_U - x_L}{\sqrt{2}}$$

Thus:

$$-\frac{1}{\sqrt{2}}(x_U - x_L) \leq x' - y' \leq \frac{1}{\sqrt{2}}(x_U - x_L)$$

Using $y - k \in [-y_{hr}, y_{hr}]$ and $x - h \in [-x_{hr}, x_{hr}]$, equations (3.4) and (3.5) yield:

$$\frac{x_L + x_U + y_L + y_U}{2} - \frac{1}{\sqrt{2}}(y_U - y_L) \leq x' + y' \leq \frac{x_L + x_U + y_L + y_U}{2} + \frac{1}{\sqrt{2}}(y_U - y_L) \tag{3.6}$$

$$\frac{x_L + x_U - y_L - y_U}{2} - \frac{1}{\sqrt{2}}(x_U - x_L) \leq x' - y' \leq \frac{x_L + x_U - y_L - y_U}{2} + \frac{1}{\sqrt{2}}(x_U - x_L) \tag{3.7}$$

Equations (3.6) and (3.7) define the extremal values of the rotated sub-region. Using these bounds we construct valid envelope formulations, yielding a set of inequalities that approximate the rotated feasible sub-region.

3.3. Convex and Concave Quadratic Estimators for Rotated Bilinear Functions. In this section, we derive valid convex under-estimators and concave over-estimators for the bilinear function over the rotated feasible region. The derivation follows from Equations (3.6) and (3.7), which define the feasible region in the rotated coordinate system. In particular, we have

$$\begin{aligned} a_1 \leq x' + y' \leq a_2, \\ b_1 \leq x' - y' \leq b_2, \end{aligned}$$

where

$$\begin{aligned} a_1 &= \frac{x_L + x_U + y_L + y_U}{2} - \frac{1}{\sqrt{2}}(y_U - y_L), \\ a_2 &= \frac{x_L + x_U + y_L + y_U}{2} + \frac{1}{\sqrt{2}}(y_U - y_L), \\ b_1 &= \frac{x_L + x_U - y_L - y_U}{2} - \frac{1}{\sqrt{2}}(x_U - x_L), \\ b_2 &= \frac{x_L + x_U - y_L - y_U}{2} + \frac{1}{\sqrt{2}}(x_U - x_L). \end{aligned}$$

From these bounds, it follows that

$$(x' + y' - a_1) \geq 0, \quad (a_2 - x' - y') \geq 0,$$

which implies

$$(x' + y' - a_1)(a_2 - x' - y') \geq 0.$$

Expanding and rearranging the above expression yields

$$x'y' \;\leq\; \frac{1}{2}\Big[- (x')^2 - (y')^2 + (x' + y')(a_1 + a_2) - a_1 a_2 \Big]. \tag{3.8}$$

Equation (3.8) defines a valid concave over-estimator for the rotated bilinear function. Similarly,

$$(x' - y' - b_1) \geq 0, \quad (b_2 - x' + y') \geq 0,$$

which implies

$$(x' - y' - b_1)(b_2 - x' + y') \geq 0.$$

Expanding and rearranging the above expression yields

$$x'y' \;\geq\; \frac{1}{2}\Big[(x')^2 + (y')^2 + (y'-x')(b_1+b_2) + b_1 b_2\Big]. \tag{3.9}$$

Equation (3.9) defines a valid convex under-estimator for the rotated bilinear function. In contrast to the four linear McCormick envelopes, the proposed relaxation yield two quadratic inequalities in the lifted space.

The main result of this paper compares the derived envelopes with the standard McCormick envelopes and proves that the proposed upper bound strictly improves upon the corresponding McCormick upper bound.

LEMMA 3.1. *Let*

$$U_{\mathrm{Mc}}(x,y) := \min\left\{x^U y + x y^L - x^U y^L,\; x^L y + x y^U - x^L y^U\right\}$$

denote the McCormick concave over-estimator of xy over $x \in [x^L, x^U]$, $y \in [y^L, y^U]$. Then

$$\max_{x\in[x^L,x^U],\, y\in[y^L,y^U]} \{U_{\mathrm{Mc}}(x,y) - xy\} = \frac{(x^U - x^L)(y^U - y^L)}{4}.$$

The maximum is attained uniquely at

$$\left(\frac{x^L + x^U}{2}, \frac{y^L + y^U}{2}\right).$$

The proof of Lemma 3.1 is a direct consequence of the convex and concave envelopes derived in McCormick [22].

THEOREM 3.2. *Let $x \in [x_L, x_U]$ and $y \in [y_L, y_U]$ and suppose that*

$$x_U - x_L > y_U - y_L.$$

Let z be an auxiliary variable representing the bilinear term $x \cdot y$.

Define the worst-case upper relaxation gap under the McCormick upper bounds as

$$\mathrm{gap}_{\mathrm{ub}}^{\mathrm{Mc}} = \max\{z - xy : z \leq x_U y + x y_L - x_U y_L,\; z \leq x_L y + x y_U - x_L y_U, x \in [x_L, x_U], y \in [y_L, y_U]\}.$$

Define the worst-case upper relaxation gap under the proposed envelope as

$$\mathrm{gap}_{\mathrm{ub}}^{\mathrm{prop}} = \max\Big\{z - x'y' : z \leq \tfrac{1}{2}\big[-x'^2 - y'^2 + (x'+y')(a_1+a_2) - a_1 a_2\big],\; a_1 \leq x'+y' \leq a_2,\; b_1 \leq x'-y' \leq b_2\Big\}.$$

Under the above assumptions,

$$\mathrm{gap}_{\mathrm{ub}}^{\mathrm{prop}} < \mathrm{gap}_{\mathrm{ub}}^{\mathrm{Mc}}.$$

Proof. By Lemma 3.1,

$$\mathrm{gap}_{\mathrm{ub}}^{\mathrm{Mc}} = \frac{(x_U - x_L)(y_U - y_L)}{4}.$$

Next, consider

$$\mathrm{gap}_{\mathrm{ub}}^{\mathrm{prop}} = \max\Big\{z - x'y' : z \leq \tfrac{1}{2}\big[-x'^2 - y'^2 + (x'+y')(a_1+a_2) - a_1 a_2\big],\; a_1 \leq x'+y' \leq a_2,\; b_1 \leq x'-y' \leq b_2\Big\}.$$

Since the objective is $z - x'y'$ and z is constrained only by an upper bound, the maximum is attained when

$$z = \tfrac{1}{2}\big[- x'^2 - y'^2 + (x' + y')(a_1 + a_2) - a_1 a_2\big].$$

Substituting this into the objective gives

$$z - x'y' = \tfrac{1}{2}\big[-x'^2 - y'^2 + (x'+y')(a_1+a_2) - a_1a_2\big] - x'y' = \tfrac{1}{2}\big[-(x'+y')^2 + (x'+y')(a_1+a_2) - a_1a_2\big].$$

Let $s = x' + y'$. Then

$$\text{gap}_{\text{ub}}^{\text{prop}} = \max_{a_1 \le s \le a_2} \tfrac{1}{2}\big[- s^2 + s(a_1 + a_2) - a_1 a_2\big].$$

This is a concave quadratic in s, maximized at

$$s^* = \frac{a_1 + a_2}{2} \tag{3.10}$$

and hence

$$\text{gap}_{\text{ub}}^{\text{prop}} = \tfrac{1}{2}\left[- \left(\frac{a_1 + a_2}{2}\right)^2 + (a_1 + a_2)\left(\frac{a_1 + a_2}{2}\right) - a_1 a_2\right] = \frac{(a_2 - a_1)^2}{8}.$$

Since

$$a_2 - a_1 = \sqrt{2}\,(y_U - y_L),$$

it follows that

$$\text{gap}_{\text{ub}}^{\text{prop}} = \frac{(y_U - y_L)^2}{4}.$$

Therefore,

$$\text{gap}_{\text{ub}}^{\text{Mc}} = \frac{(x_U - x_L)(y_U - y_L)}{4} \quad \text{and} \quad \text{gap}_{\text{ub}}^{\text{prop}} = \frac{(y_U - y_L)^2}{4}.$$

Since $x_U - x_L > y_U - y_L$, we obtain

$$\frac{(x_U - x_L)(y_U - y_L)}{4} > \frac{(y_U - y_L)^2}{4},$$

which proves that $\text{gap}_{\text{ub}}^{\text{Mc}} > \text{gap}_{\text{ub}}^{\text{prop}}$. □

Theorem 3.2 establishes that the proposed concave quadratic over-estimator has a strictly smaller worst-case upper relaxation gap than the McCormick concave relaxation whenever $x^U - x^L > y^U - y^L$. Moreover, the maximizer of $\text{gap}_{\text{ub}}^{\text{prop}}$ is independent of b_1 and b_2, and is attained at

$$x' + y' = \frac{a_1 + a_2}{2},$$

which corresponds to a ridge in the middle of the elongated axis of the rotated feasible sub-region.

COROLLARY 3.3 (Argmax structure and containment). *Let $x \in [x_L, x_U]$ and $y \in [y_L, y_U]$, and suppose that*

$$x_U - x_L > y_U - y_L.$$

Let P_M and P_P denote the sets of spatial locations attaining the worst-case McCormick and proposed upper-relaxation gaps, respectively.

Then the following hold:

(i) The McCormick problem has the unique maximizer

$$x_M^* = \frac{x_L + x_U}{2}, \qquad y_M^* = \frac{y_L + y_U}{2},$$

(ii) The argmax set of the proposed problem is

$$P_P = \left\{ (x', y', z) : x' + y' = \frac{a_1 + a_2}{2},\ b_1 \le x' - y' \le b_2,\ z = \tfrac{1}{2}\big[- x'^2 - y'^2 + (a_1 + a_2)(x' + y') - a_1 a_2 \big] \right\}.$$

(iii) The McCormick maximizer belongs to the proposed argmax set:

$$(x_M^*, y_M^*) \in P_P.$$

(iv) Consequently,

$$P_M = \{(x_M^*, y_M^*)\} \subseteq P_P.$$

Proof. From the proof of Theorem 3.2, and using equation (3.10) the objective of the proposed problem is maximized uniquely at

$$s^* = \frac{a_1 + a_2}{2}.$$

Hence any maximizer must satisfy

$$x' + y' = \frac{a_1 + a_2}{2}.$$

Since the feasible region in the rotated coordinates is defined by

$$a_1 \le x' + y' \le a_2, \qquad b_1 \le x' - y' \le b_2,$$

it follows that for any $t = x' - y' \in [b_1, b_2]$, the pair

$$x' = \frac{s^* + t}{2}, \qquad y' = \frac{s^* - t}{2}$$

is feasible. Therefore, all such points achieve the same objective value, and the argmax set of the proposed problem is

$$P_P = \left\{ (x', y', z) : x + y = \frac{a_1 + a_2}{2},\ b_1 \le x' - y' \le b_2,\ z = \tfrac{1}{2}[-x'^2 - y'^2 + (a_1 + a_2)(x' + y') - a_1 a_2] \right\}.$$

From Lemma 3.1, the McCormick problem has the unique maximizer

$$x_M^* = \frac{x_L + x_U}{2}, \qquad y_M^* = \frac{y_L + y_U}{2}.$$

Using the identities $a_1 + a_2 = x_L + x_U + y_L + y_U$, we obtain

$$x_M^* + y_M^* = \frac{a_1 + a_2}{2}.$$

Moreover,

$$x_M^* - y_M^* = \frac{x_L + x_U - y_L - y_U}{2} \in [b_1, b_2].$$

Thus,

$$(x_M^*, y_M^*) \in P_P.$$

Since the McCormick maximizer is unique, it follows that

$$P_M = \{(x_M^*, y_M^*)\} \subseteq P_P. \qquad \square$$

Corollary 3.3 shows that while the McCormick relaxation yields a unique maximizer, the proposed relaxation admits a continuum of maximizers along the line $x' + y' = \frac{a_1+a_2}{2}$. This indicates that the proposed envelope aligns more closely with the geometry of the bilinear surface, while retaining the McCormick solution within its optimal set.

The main results can be summarized as follows:

1. Theorem 3.2 establishes that the proposed upper envelope yields a strictly smaller worst-case relaxation gap than the McCormick envelope whenever $x_U - x_L > y_U - y_L$, demonstrating its improved tightness.
2. Corollary 3.3 characterizes the structure of the maximizers, showing that while the McCormick relaxation admits a unique maximizer, the proposed relaxation yields a continuum of optimal solutions along the line $x' + y' = \frac{a_1+a_2}{2}$, and that the McCormick maximizer is contained within this set.

It is worth noting that when $x_U - x_L > y_U - y_L$, the proposed approach yields strictly tighter upper bounds compared to the standard McCormick envelopes, while the corresponding lower bounds are not guaranteed to improve upon the McCormick lower bounds. Conversely, a 45° anti-clockwise rotation can be employed to derive tighter lower bounds than the McCormick lower bounds.

Without loss of generality, for the case $y_U - y_L > x_U - x_L$, the rotated formulation yields the following convex under-estimator:

$$x'y' \geq \frac{1}{2}\big[x'^2 + y'^2 + (y' - x')(d_1 + d_2) + d_1 d_2\big],$$

where

$$d_1 = \frac{x_L + x_U - y_L - y_U}{2} - \frac{1}{\sqrt{2}}(y_U - y_L), \qquad d_2 = \frac{x_L + x_U - y_L - y_U}{2} + \frac{1}{\sqrt{2}}(y_U - y_L).$$

and the following concave over-estimator:

$$x'y' \leq \frac{1}{2}\big[-(x'^2 + y'^2) + (x' + y')(c_1 + c_2) - c_1 c_2\big],$$

where

$$c_1 = \frac{x_L + x_U + y_L + y_U}{2} - \frac{1}{\sqrt{2}}(x_U - x_L), \qquad c_2 = \frac{x_L + x_U + y_L + y_U}{2} + \frac{1}{\sqrt{2}}(x_U - x_L).$$

This convex lower bound is strictly tighter than the corresponding McCormick lower bounds.

These results highlight that the strength of the proposed relaxations depends on the relative scaling of the variable domains. By exploiting this asymmetry, the rotated feasible region better aligns with the curvature of the bilinear surface, leading to directionally improved relaxations—upper or lower bounds depending on the orientation of the rotation. Finally, when $x^U - x^L = y^U - y^L$, the corresponding worst-case relaxation gaps of the proposed and McCormick formulations are equal; hence no strict improvement in worst-case gap is obtained from the rotation.

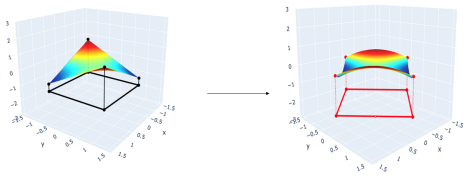


Fig. 6: Surface plot for Bilinear terms under different geometric orientations

4. Range Analysis of Bilinear Terms Under Rotation. In this section, we analyze the range of the bilinear function over the original rectangular region and compare it with the range obtained after a 45° clockwise rotation about the center of the region. Fig 6 illustrates the surface of the bilinear term over both the original and rotated sub-regions. We observe that the rotated sub-region exhibits a comparatively *flatter* surface. This observation motivates the following question: when and why does the rotated surface appear flatter? This forms the basis for the range analysis developed in this section.

For the original rectangular region, the maximum and minimum of the bilinear function occur at the corner points of the feasible region. In contrast, for the rotated sub-regions, the extrema may occur either at the vertices or along the edges (ridges) of the feasible region. Specifically, we consider

$$\Delta_{\text{orig}} := \max(xy) - \min(xy),$$

and

$$\begin{aligned} \Delta_{rot} &= \max(x_1'y_1') - \min(x_2'y_2') \\ a_1 &\le x_1' + y_1' \le a_2 \\ b_1 &\le x_1' - y_1' \le b_2 \\ a_1 &\le x_2' + y_2' \le a_2 \\ b_1 &\le x_2' - y_2' \le b_2 \end{aligned}$$

4.1. Preliminaries. Let

$$x \in [x_L, x_U], \qquad y \in [y_L, y_U],$$

with

$$\Delta x := x_U - x_L, \qquad \Delta y := y_U - y_L, \qquad \Delta x > \Delta y > 0.$$

Define the center and half-widths as

$$h := \frac{x_L + x_U}{2}, \qquad k := \frac{y_L + y_U}{2},$$

$$x_{hr} := \frac{\Delta x}{2}, \qquad y_{hr} := \frac{\Delta y}{2}$$

4.2. Range of the Bilinear Function Under Rotation. The range of the bilinear function in the rotated space is defined as,

$$\begin{aligned} \Delta_{rot} &= \max(x'y') - \min(x'y') \\ a_1 &\le x' + y' \le a_2 \\ b_1 &\le x' - y' \le b_2 \end{aligned}$$

where a_1, a_2, b_1 and b_2 are defined in equations (3.6) and (3.7). The above problem is separable in nature and can be defined as two separate optimization problems.

Consider the optimization problem

$$\begin{aligned} z_{\max} := \max_{x',y'} \quad & x'y' \\ \text{s.t.} \quad & a_1 \le x' + y' \le a_2, \\ & b_1 \le x' - y' \le b_2, \end{aligned} \tag{4.1}$$

where

$$a_1 < a_2, \qquad b_1 < b_2.$$

4.3. KKT Conditions. To use the standard KKT convention for minimization problems with inequalities of the form $g_i \le 0$, problem (4.1) is equivalently expressed as

$$\begin{aligned} \min_{x',y'} \quad & -x'y' \\ \text{s.t.} \quad & g_1(x',y') := a_1 - x' - y' \le 0, \\ & g_2(x',y') := x' + y' - a_2 \le 0, \\ & g_3(x',y') := b_1 - x' + y' \le 0, \\ & g_4(x',y') := x' - y' - b_2 \le 0. \end{aligned} \tag{4.2}$$

Let $\mu_i \ge 0$, $i = 1, \ldots, 4$, be the Lagrange multiplier associated with g_i. The Lagrangian is

$$\begin{aligned} \mathcal{L}(x', y', \mu) = & -x'y' + \mu_1(a_1 - x' - y') + \mu_2(x' + y' - a_2) \\ & + \mu_3(b_1 - x' + y') + \mu_4(x' - y' - b_2). \end{aligned} \tag{4.3}$$

The stationarity conditions derived from the Lagrangian are

$$-y' - \mu_1 + \mu_2 - \mu_3 + \mu_4 = 0, \tag{4.4a}$$

$$-x' - \mu_1 + \mu_2 + \mu_3 - \mu_4 = 0. \tag{4.4b}$$

Adding and subtracting (4.4a) and (4.4b) gives

$$x' + y' = 2(\mu_2 - \mu_1), \tag{4.5a}$$

$$x' - y' = 2(\mu_3 - \mu_4). \tag{4.5b}$$

The remaining KKT conditions are primal feasibility,

$$a_1 \le x' + y' \le a_2, \qquad b_1 \le x' - y' \le b_2, \tag{4.6}$$

dual feasibility,

$$\mu_i \ge 0, \qquad i = 1, \ldots, 4, \tag{4.7}$$

and complementary slackness,

$$\mu_1(a_1 - x' - y') = 0, \tag{4.8a}$$

$$\mu_2(x' + y' - a_2) = 0, \tag{4.8b}$$

$$\mu_3(b_1 - x' + y') = 0, \tag{4.8c}$$

$$\mu_4(x' - y' - b_2) = 0. \tag{4.8d}$$

4.4. Admissible Active Sets. Let C_i denote the boundary $g_i(x', y') = 0$. Although four inequalities generate $2^4 = 16$ formal active-set combinations, only nine are feasible.

The constraints C_1 and C_2 cannot be active simultaneously, because this would require

$$x' + y' = a_1 \qquad \text{and} \qquad x' + y' = a_2,$$

which is impossible when $a_1 < a_2$. Similarly, C_3 and C_4 cannot be active simultaneously, because this would require

$$x' - y' = b_1 \qquad \text{and} \qquad x' - y' = b_2,$$

which is impossible when $b_1 < b_2$.

Furthermore, every subset of three or four constraints necessarily contains either the incompatible pair $\{C_1, C_2\}$ or the incompatible pair $\{C_3, C_4\}$. Hence, no active set of cardinality three or four is feasible. The complete collection of admissible active sets is therefore

$$\varnothing, \tag{4.9}$$

the four singleton sets

$$\{C_1\}, \quad \{C_2\}, \quad \{C_3\}, \quad \{C_4\}, \tag{4.10}$$

and the four compatible pairs

$$\{C_1, C_3\}, \quad \{C_1, C_4\}, \quad \{C_2, C_3\}, \quad \{C_2, C_4\}. \tag{4.11}$$

Geometrically, these cases correspond, respectively, to an interior point, the relative interiors of the four edges, and the four vertices of the parallelogram.

4.5. KKT Candidate Points.

4.5.1. Interior point. If no constraint is active, complementary slackness gives

$$\mu_1 = \mu_2 = \mu_3 = \mu_4 = 0.$$

The stationarity conditions then imply

$$x' = y' = 0.$$

Thus, the only interior KKT point is the origin, provided

$$a_1 < 0 < a_2, \qquad b_1 < 0 < b_2.$$

The Hessian of the original objective $f(x', y') = x'y'$ is

$$\nabla^2 f(x', y') = \begin{bmatrix} 0 & 1 \\ 1 & 0 \end{bmatrix}, \tag{4.12}$$

whose eigenvalues are 1 and -1. Hence, the origin is a saddle point and cannot be a local maximum.

4.5.2. Edges $x' + y' = a_i$. Suppose first that only C_1 is active. Then

$$x' + y' = a_1, \qquad \mu_2 = \mu_3 = \mu_4 = 0.$$

Stationarity gives

$$x' = y' = -\mu_1.$$

Therefore,

$$E_1 = \left(\frac{a_1}{2}, \frac{a_1}{2}\right), \qquad \mu_1 = -\frac{a_1}{2}. \tag{4.13}$$

Dual feasibility requires $a_1 \leq 0$. Moreover, because $x' - y' = 0$, feasibility requires

$$b_1 \leq 0 \leq b_2.$$

The point lies in the relative interior of the edge when $b_1 < 0 < b_2$. Its objective value is

$$f(E_1) = \frac{a_1^2}{4}. \tag{4.14}$$

Similarly, if only C_2 is active, then

$$E_2 = \left(\frac{a_2}{2}, \frac{a_2}{2}\right), \qquad \mu_2 = \frac{a_2}{2}. \tag{4.15}$$

This point is a KKT candidate when

$$a_2 \geq 0, \qquad b_1 \leq 0 \leq b_2,$$

and

$$f(E_2) = \frac{a_2^2}{4}. \tag{4.16}$$

To classify these stationary points, restrict the objective to an edge

$$x' + y' = a_i.$$

Substituting $y' = a_i - x'$ gives

$$f(x', a_i - x') = a_i x' - (x')^2.$$

Therefore,

$$\frac{d^2}{d(x')^2}\left(a_i x' - (x')^2\right) = -2 < 0.$$

Hence, whenever E_i is feasible, it is the unique maximizer of the objective along the corresponding edge.

4.5.3. Edges $x' - y' = b_j$. If only C_3 is active, stationarity gives

$$F_1 = \left(\frac{b_1}{2}, -\frac{b_1}{2}\right), \qquad \mu_3 = \frac{b_1}{2}. \tag{4.17}$$

Thus, dual feasibility requires $b_1 \geq 0$, while primal feasibility requires

$$a_1 \leq 0 \leq a_2.$$

If only C_4 is active, stationarity gives

$$F_2 = \left(\frac{b_2}{2}, -\frac{b_2}{2}\right), \qquad \mu_4 = -\frac{b_2}{2}. \tag{4.18}$$

Thus, dual feasibility requires $b_2 \le 0$, while primal feasibility again requires

$$a_1 \le 0 \le a_2.$$

These points cannot be local maxima. Indeed, on an edge

$$x' - y' = b_j,$$

substitution of $y' = x' - b_j$ gives

$$f(x', x' - b_j) = (x')^2 - b_j x',$$

and hence

$$\frac{d^2}{d(x')^2}\left((x')^2 - b_j x'\right) = 2 > 0.$$

Therefore, F_j is the unique minimum of the objective along the corresponding edge.

Consequently, the only possible nonvertex local maximizers are E_1 and E_2.

4.5.4. Vertices. For $i, j \in \{1, 2\}$, let P_{ij} denote the vertex satisfying

$$x' + y' = a_i, \qquad x' - y' = b_j.$$

Solving these equations gives

$$P_{ij} = \left(\frac{a_i + b_j}{2}, \frac{a_i - b_j}{2}\right). \tag{4.19}$$

The objective value at P_{ij} is

$$f(P_{ij}) = \frac{a_i^2 - b_j^2}{4}. \tag{4.20}$$

The associated KKT multipliers and dual-feasibility conditions are summarized in Table 1.

Table 1: KKT conditions at the vertices of the rotated region.

Vertex	Nonzero multipliers	Dual-feasibility conditions
P_{11}	$\mu_1 = -a_1/2, \quad \mu_3 = b_1/2$	$a_1 \le 0, \quad b_1 \ge 0$
P_{12}	$\mu_1 = -a_1/2, \quad \mu_4 = -b_2/2$	$a_1 \le 0, \quad b_2 \le 0$
P_{21}	$\mu_2 = a_2/2, \quad \mu_3 = b_1/2$	$a_2 \ge 0, \quad b_1 \ge 0$
P_{22}	$\mu_2 = a_2/2, \quad \mu_4 = -b_2/2$	$a_2 \ge 0, \quad b_2 \le 0$

4.6. Global Solution. The KKT conditions identify all possible local maximizers, but they do not, by themselves, establish global optimality because $f(x', y') = x'y'$ is neither concave nor convex. The global maximizer can be obtained by exploiting the identity

$$4x'y' = (x' + y')^2 - (x' - y')^2. \tag{4.21}$$

Define

$$u = x' + y', \qquad v = x' - y'. \tag{4.22}$$

The transformation is nonsingular, with inverse

$$x' = \frac{u + v}{2}, \qquad y' = \frac{u - v}{2}. \tag{4.23}$$

Under this transformation, the feasible parallelogram becomes the rectangle

$$u \in [a_1, a_2], \qquad v \in [b_1, b_2], \tag{4.24}$$

and the objective becomes

$$x'y' = \frac{u^2 - v^2}{4}. \tag{4.25}$$

Because u and v vary independently over their respective intervals,

$$\max_{\substack{u\in[a_1,a_2]\\ v\in[b_1,b_2]}} \frac{u^2 - v^2}{4} = \frac{1}{4}\left[\max_{u\in[a_1,a_2]} u^2 - \min_{v\in[b_1,b_2]} v^2\right]. \tag{4.26}$$

Define

$$\mathcal{A}^* := \operatorname*{arg\,max}_{A\in\{a_1,a_2\}} A^2 \tag{4.27}$$

and

$$B^* := \operatorname{proj}_{[b_1,b_2]}(0) = \begin{cases} 0, & b_1 \le 0 \le b_2, \\ b_1, & b_1 > 0, \\ b_2, & b_2 < 0. \end{cases} \tag{4.28}$$

PROPOSITION 4.1. *Every global maximizer of* (4.1) *is of the form*

$$\boxed{(x'^*, y'^*) = \left(\frac{A^* + B^*}{2}, \frac{A^* - B^*}{2}\right), \qquad A^* \in \mathcal{A}^*.} \tag{4.29}$$

The global optimal value is

$$\boxed{z_{\max} = \frac{1}{4}\left[\max\{a_1^2, a_2^2\} - \operatorname{dist}(0, [b_1, b_2])^2\right].} \tag{4.30}$$

Proof. The maximum of u^2 over the interval $[a_1, a_2]$ is attained at an endpoint, so

$$\max_{u\in[a_1,a_2]} u^2 = \max\{a_1^2, a_2^2\}.$$

The minimum of v^2 over $[b_1, b_2]$ is attained at the projection of the origin onto that interval. Hence,

$$\min_{v\in[b_1,b_2]} v^2 = \operatorname{dist}(0,[b_1,b_2])^2 .$$

Substitution into (4.26) proves (4.30). The optimizer follows from the inverse transformation (4.23). ∎

Equivalently, the global optimal value can be written as

$$z_{\max} = \begin{cases} \dfrac{1}{4}\max\{a_1^2, a_2^2\}, & b_1 \le 0 \le b_2, \\ \dfrac{1}{4}\left[\max\{a_1^2, a_2^2\} - b_1^2\right], & b_1 > 0, \\ \dfrac{1}{4}\left[\max\{a_1^2, a_2^2\} - b_2^2\right], & b_2 < 0. \end{cases} \tag{4.31}$$

If

$$b_1 < 0 < b_2,$$

then $B^* = 0$, and every global maximizer satisfies

$$x'^* = y'^*.$$

The maximizer therefore lies in the relative interior of one of the edges $x' + y' = a_i$. If $b_1 = 0$ or $b_2 = 0$, the same formula gives a vertex. If

$$0 \notin [b_1, b_2],$$

then B^* is one of the interval endpoints and the global maximizer is necessarily a vertex.

We next consider

$$\begin{aligned} z_{\min} := \min_{x',y'} \quad & x'y' \\ \text{s.t.} \quad & a_1 \le x' + y' \le a_2, \\ & b_1 \le x' - y' \le b_2. \end{aligned} \tag{4.32}$$

The feasible region, constraint functions g_i, boundary sets C_i, and admissible active sets are identical to those introduced above. In particular, the only admissible active sets are

$$\varnothing, \quad \{C_1\},\{C_2\},\{C_3\},\{C_4\}, \quad \{C_1,C_3\},\{C_1,C_4\},\{C_2,C_3\},\{C_2,C_4\}.$$

4.7. KKT conditions for minimizing $x'y'$. Let $\mu_i \ge 0$ denote the multiplier associated with g_i, $i = 1,\dots,4$. The Lagrangian for (4.32) is

$$\begin{aligned} \mathcal{L}_{\min}(x',y',\mu) = x'y' &+ \mu_1(a_1 - x' - y') + \mu_2(x' + y' - a_2) \\ &+ \mu_3(b_1 - x' + y') + \mu_4(x' - y' - b_2). \end{aligned} \tag{4.33}$$

The stationarity conditions are

$$y' - \mu_1 + \mu_2 - \mu_3 + \mu_4 = 0, \tag{4.34a}$$
$$x' - \mu_1 + \mu_2 + \mu_3 - \mu_4 = 0. \tag{4.34b}$$

Equivalently,

$$x' + y' = 2(\mu_1 - \mu_2), \tag{4.35a}$$
$$x' - y' = 2(\mu_4 - \mu_3). \tag{4.35b}$$

These equations are supplemented by primal feasibility,

$$a_1 \le x' + y' \le a_2, \qquad b_1 \le x' - y' \le b_2,$$

dual feasibility,

$$\mu_i \ge 0, \qquad i = 1, \dots, 4,$$

and complementary slackness,

$$\mu_1(a_1 - x' - y') = 0, \tag{4.36a}$$
$$\mu_2(x' + y' - a_2) = 0, \tag{4.36b}$$
$$\mu_3(b_1 - x' + y') = 0, \tag{4.36c}$$
$$\mu_4(x' - y' - b_2) = 0. \tag{4.36d}$$

4.8. KKT candidates for global minima. Retain the candidate notation introduced in the maximization analysis:

$$O := (0, 0), \tag{4.37}$$
$$E_i := \left(\frac{a_i}{2}, \frac{a_i}{2}\right), \qquad i \in \{1, 2\}, \tag{4.38}$$
$$F_j := \left(\frac{b_j}{2}, -\frac{b_j}{2}\right), \qquad j \in \{1, 2\}, \tag{4.39}$$
$$P_{ij} := \left(\frac{a_i + b_j}{2}, \frac{a_i - b_j}{2}\right), \qquad i, j \in \{1, 2\}. \tag{4.40}$$

Their objective values are

$$f(O) = 0, \tag{4.41}$$
$$f(E_i) = \frac{a_i^2}{4}, \tag{4.42}$$
$$f(F_j) = -\frac{b_j^2}{4}, \tag{4.43}$$
$$f(P_{ij}) = \frac{a_i^2 - b_j^2}{4}. \tag{4.44}$$

The KKT admissibility conditions for the minimization problem are summarized in Table 2.

The edge classifications follow from the one-dimensional restrictions already obtained in the maximization analysis. On $x' + y' = a_i$,

$$x'y' = a_i x' - (x')^2,$$

Table 2: KKT candidates for the minimization of $x'y'$.

Active set	Candidate	Nonzero multipliers	Admissibility conditions	Classification
$\varnothing$	O	None	$a_1 < 0 < a_2,\ b_1 < 0 < b_2$	Saddle point
$\{C_1\}$	E_1	$\mu_1 = a_1/2$	$a_1 \geq 0,\ b_1 < 0 < b_2$	Maximum on C_1
$\{C_2\}$	E_2	$\mu_2 = -a_2/2$	$a_2 \leq 0,\ b_1 < 0 < b_2$	Maximum on C_2
$\{C_3\}$	F_1	$\mu_3 = -b_1/2$	$b_1 \leq 0,\ a_1 < 0 < a_2$	Minimum on C_3
$\{C_4\}$	F_2	$\mu_4 = b_2/2$	$b_2 \geq 0,\ a_1 < 0 < a_2$	Minimum on C_4
$\{C_1, C_3\}$	P_{11}	$\mu_1 = a_1/2,\ \mu_3 = -b_1/2$	$a_1 \geq 0,\ b_1 \leq 0$	Vertex candidate
$\{C_1, C_4\}$	P_{12}	$\mu_1 = a_1/2,\ \mu_4 = b_2/2$	$a_1 \geq 0,\ b_2 \geq 0$	Vertex candidate
$\{C_2, C_3\}$	P_{21}	$\mu_2 = -a_2/2,\ \mu_3 = -b_1/2$	$a_2 \leq 0,\ b_1 \leq 0$	Vertex candidate
$\{C_2, C_4\}$	P_{22}	$\mu_2 = -a_2/2,\ \mu_4 = b_2/2$	$a_2 \leq 0,\ b_2 \geq 0$	Vertex candidate

which is strictly concave. Hence E_i is an edge maximum and cannot be a local minimum in the relative interior of that edge.

On $x' - y' = b_j$,

$$x'y' = (x')^2 - b_j x',$$

which is strictly convex. Hence F_j is the unique minimum on the corresponding edge.

The interior point O is a saddle point. Therefore, every global minimizer is either F_1, F_2, or one of the four vertices P_{ij}.

4.9. Global minimizer. For any feasible point, let

$$A := x' + y', \qquad B := x' - y'. \tag{4.45}$$

Then

$$x' = \frac{A+B}{2}, \qquad y' = \frac{A-B}{2}, \tag{4.46}$$

and consequently

$$x'y' = \frac{A^2 - B^2}{4}. \tag{4.47}$$

Since

$$A \in [a_1, a_2], \qquad B \in [b_1, b_2]$$

independently, minimizing $x'y'$ requires selecting the feasible A having the smallest absolute value and the feasible B having the largest absolute value.

Define

$$A^\star := \operatorname{proj}_{[a_1,a_2]}(0) = \begin{cases} 0, & a_1 \leq 0 \leq a_2, \\ a_1, & a_1 > 0, \\ a_2, & a_2 < 0, \end{cases} \tag{4.48}$$

and

$$\mathcal{B}^\star := \operatorname*{arg\,max}_{B \in \{b_1, b_2\}} B^2. \tag{4.49}$$

Thus,

$$\mathcal{B}^\star = \begin{cases} \{b_1\}, & b_1^2 > b_2^2, \\ \{b_2\}, & b_2^2 > b_1^2, \\ \{b_1, b_2\}, & b_1^2 = b_2^2. \end{cases} \tag{4.50}$$

PROPOSITION 4.2. *Every global minimizer of* (4.32) *is of the form*

$$\boxed{(x'^\star, y'^\star) = \left(\frac{A^\star + B^\star}{2}, \frac{A^\star - B^\star}{2}\right), \qquad B^\star \in \mathcal{B}^\star.} \tag{4.51}$$

The global minimum is

$$\boxed{z_{\min} = \frac{1}{4}\left[\operatorname{dist}(0, [a_1, a_2])^2 - \max\{b_1^2, b_2^2\}\right].} \tag{4.52}$$

For every feasible $A \in [a_1, a_2]$ and $B \in [b_1, b_2]$,

$$A^2 \geq (A^\star)^2$$

and, for any $B^\star \in \mathcal{B}^\star$,

$$B^2 \leq (B^\star)^2.$$

Therefore,

$$\frac{A^2 - B^2}{4} \geq \frac{(A^\star)^2 - (B^\star)^2}{4}. \tag{4.53}$$

Equivalently,

$$z_{\min} = \begin{cases} -\dfrac{1}{4}\max\{b_1^2, b_2^2\}, & a_1 \leq 0 \leq a_2, \\ \dfrac{1}{4}\left[a_1^2 - \max\{b_1^2, b_2^2\}\right], & a_1 > 0, \\ \dfrac{1}{4}\left[a_2^2 - \max\{b_1^2, b_2^2\}\right], & a_2 < 0. \end{cases} \tag{4.54}$$

where

$$\operatorname{dist}(0, [a_1, a_2]) := \min_{A \in [a_1, a_2]} |A|.$$

Hence,

$$\operatorname{dist}(0, [a_1, a_2])^2 = \begin{cases} 0, & a_1 \leq 0 \leq a_2, \\ a_1^2, & a_1 > 0, \\ a_2^2, & a_2 < 0. \end{cases}$$

Therefore, (4.52) can equivalently be written as

If $a_1 < 0 < a_2$, then $A^\star = 0$, and every global minimizer satisfies

$$x'^\star = -y'^\star.$$

Such a minimizer lies in the relative interior of C_3 or C_4, depending on which of $|b_1|$ and $|b_2|$ is larger. If $a_1 = 0$ or $a_2 = 0$, the corresponding minimizer is a vertex. If $0 \notin [a_1, a_2]$, every global minimizer is a vertex.

5. Comparison of the Bilinear Ranges. Let

$$\mathcal{R}_{\text{orig}} = [x^L, x^U] \times [y^L, y^U]$$

denote the original axis-aligned rectangle, and let

$$\mathcal{R}_{\text{rot}} = \{(x', y') : a_1 \le x' + y' \le a_2,\ b_1 \le x' - y' \le b_2\}$$

Throughout this section, assume

$$x_{hr} > y_{hr} \tag{5.1}$$

For notational convenience, define

$$S := |h + k|, \qquad D := |h - k|, \qquad \alpha := \sqrt{2}\, y_{hr}, \qquad \beta := \sqrt{2}\, x_{hr}. \tag{5.2}$$

Under (5.1),

$$\beta > \alpha.$$

5.1. Range over the rotated region. Define the range of the bilinear term over the rotated region by

$$\Delta_{\text{rot}} := \max_{(x',y') \in \mathcal{R}_{\text{rot}}} x'y' - \min_{(x',y') \in \mathcal{R}_{\text{rot}}} x'y'. \tag{5.3}$$

The preceding maximization and minimization analyses give

$$z^{\text{rot}}_{\max} = \frac{1}{4}\left[(S + \alpha)^2 - (D - \beta)_+^2\right], \tag{5.4}$$

and

$$z^{\text{rot}}_{\min} = \frac{1}{4}\left[(S - \alpha)_+^2 - (D + \beta)^2\right], \tag{5.5}$$

where

$$(t)_+ := \max\{t, 0\}.$$

Subtracting (5.5) from (5.4) yields the following result.

PROPOSITION 5.1. *The exact range of $x'y'$ over $\mathcal{R}_{\text{rot}}$ is*

$$\boxed{\begin{aligned}\Delta_{\text{rot}} = \frac{1}{4}\Big[&(S + \alpha)^2 - (S - \alpha)_+^2 \\ &+ (D + \beta)^2 - (D - \beta)_+^2\Big].\end{aligned}} \tag{5.6}$$

Equivalently,

$$\boxed{\begin{aligned}\Delta_{\text{rot}} = \frac{1}{4}\Big[&\left(|h + k| + \sqrt{2}\, y_{hr}\right)^2 \\ &- \left(|h + k| - \sqrt{2}\, y_{hr}\right)_+^2 \\ &+ \left(|h - k| + \sqrt{2}\, x_{hr}\right)^2 \\ &- \left(|h - k| - \sqrt{2}\, x_{hr}\right)_+^2\Big].\end{aligned}} \tag{5.7}$$

673 To expose the structure of (5.6), define

674 (5.8) $$\psi(t,r) := \frac{1}{4}\left[(t+r)^2 - (t-r)_+^2\right], \qquad t, r \geq 0.$$

675 Then

676 (5.9) $$\psi(t,r) = \begin{cases} \dfrac{(t+r)^2}{4}, & 0 \leq t \leq r, \\ tr, & t > r. \end{cases}$$

677 Consequently,

678 (5.10) $$\boxed{\Delta_{\text{rot}} = \psi(S,\alpha) + \psi(D,\beta).}$$

679 The complete piecewise representation is therefore

680 (5.11) $$\Delta_{\text{rot}} = \begin{cases} \dfrac{(S+\alpha)^2 + (D+\beta)^2}{4}, & S \leq \alpha, \quad D \leq \beta, \\ \dfrac{(S+\alpha)^2}{4} + D\beta, & S \leq \alpha, \quad D > \beta, \\ S\alpha + \dfrac{(D+\beta)^2}{4}, & S > \alpha, \quad D \leq \beta, \\ S\alpha + D\beta, & S > \alpha, \quad D > \beta. \end{cases}$$

681 The conditions appearing in (5.11) also identify the locations of the extrema. In
682 particular,

683 $$D \leq \beta \quad \Longleftrightarrow \quad 0 \in [b_1, b_2],$$

684 in which case a global maximizer satisfies $x' = y'$. Similarly,

685 $$S \leq \alpha \quad \Longleftrightarrow \quad 0 \in [a_1, a_2],$$

686 in which case a global minimizer satisfies $x' = -y'$.

687 **5.2. Range over the original rectangular region.** Define

688 (5.12) $$\Delta_{\text{orig}} := \max_{(x,y)\in\mathcal{R}_{\text{orig}}} xy - \min_{(x,y)\in\mathcal{R}_{\text{orig}}} xy.$$

689 For a fixed value of x, the function xy is affine in y; hence, its maximum and
690 minimum over $[y_L, y_U]$ occur at y_L or y_U. After restricting y to either endpoint,
691 the resulting function is affine in x, and its extrema occur at x_L or x_U. Thus, both
692 extrema over $\mathcal{R}_{\text{orig}}$ occur at vertices.
693 Define the four corner values by

694 (5.13) $$\begin{aligned} q_{LL} &:= x_L y_L, \quad q_{LU} := x_L y_U, \\ q_{UL} &:= x_U y_L, \quad q_{UU} := x_U y_U. \end{aligned}$$

695 It follows immediately that

696 (5.14) $$\boxed{\Delta_{\text{orig}} = \max\{q_{LL}, q_{LU}, q_{UL}, q_{UU}\} - \min\{q_{LL}, q_{LU}, q_{UL}, q_{UU}\}.}$$

697 The next proposition gives an equivalent closed-form expression in terms of the
698 midpoint and half-range parameters.

PROPOSITION 5.2. *Let*

$$P := x_{hr}|k|, \qquad Q := y_{hr}|h|, \qquad H := x_{hr}y_{hr}. \tag{5.15}$$

Then

$$\boxed{\Delta_{\text{orig}} = 2\max\{P+Q,\ P+H,\ Q+H\}.} \tag{5.16}$$

Equivalently,

$$\boxed{\Delta_{\text{orig}} = 2\left(P+Q+H-\min\{P,Q,H\}\right).} \tag{5.17}$$

In terms of h, k, x_{hr}, *and* y_{hr},

$$\boxed{\begin{aligned}\Delta_{\text{orig}} = 2\max\big\{&x_{hr}|k| + h_y|h|,\\ &x_{hr}|k| + x_{hr}y_{hr},\\ &y_{hr}|h| + x_{hr}y_{hr}\big\}.\end{aligned}} \tag{5.18}$$

Proof. Write

$$x = h + \sigma x_{hr}, \qquad y = k + \tau y_{hr}, \qquad \sigma, \tau \in \{-1, 1\}.$$

At a vertex,

$$xy = h \cdot k + \sigma x_{hr}k + \tau y_{hr}h + \sigma\tau x_{hr}y_{hr}.$$

Let

$$E := x_{hr}k, \qquad F := y_{hr}h, \qquad G := x_{hr}y_{hr}.$$

After subtracting the common term $h \cdot k$, the four corner values are

$$E + F + G, \qquad E - F - G, \qquad -E + F - G, \qquad -E - F + G.$$

The range equals the largest absolute difference between two of these quantities. The six pairwise differences, divided by 2, have absolute values

$$|E+F|, \quad |E-F|, \quad |E+G|, \quad |E-G|, \quad |F+G|, \quad |F-G|.$$

Using

$$\max\{|u+v|, |u-v|\} = |u| + |v|,$$

and noting that $G \geq 0$, one obtains

$$\Delta_{\text{orig}} = 2\max\{|E|+|F|,\ |E|+G,\ |F|+G\}.$$

Since

$$|E| = x_{hr}|k| = P, \qquad |F| = y_{hr}|h| = Q, \qquad G = H,$$

equation (5.16) follows. The identity

$$\max\{P+Q, P+H, Q+H\} = P+Q+H-\min\{P,Q,H\}$$

gives (5.17). ∎

5.3. Exact comparison of the two ranges. Define the range difference

$$\Gamma := \Delta_{\text{rot}} - \Delta_{\text{orig}}. \tag{5.19}$$

Using Propositions 5.1 and 5.2,

$$\boxed{\begin{aligned}\Gamma = {} & \psi(S,\alpha) + \psi(D,\beta) \\ & - 2\max\{P+Q,\ P+H,\ Q+H\}.\end{aligned}} \tag{5.20}$$

Equivalently,

$$\boxed{\begin{aligned}\Gamma = {} & \psi(S,\alpha) + \psi(D,\beta) \\ & - 2\left(P+Q+H-\min\{P,Q,H\}\right).\end{aligned}} \tag{5.21}$$

Equivalently, in terms of the original variable bounds,

$$\boxed{\begin{aligned}\Gamma = {} & \frac{1}{16}\Bigg[\left(\left|x^U+x^L+y^U+y^L\right| + \sqrt{2}\,(y^U-y^L)\right)^2 \\ & \quad - \left(\left|x^U+x^L+y^U+y^L\right| - \sqrt{2}\,(y^U-y^L)\right)_+^2 \\ & \quad + \left(\left|x^U+x^L-y^U-y^L\right| + \sqrt{2}\,(x^U-x^L)\right)^2 \\ & \quad - \left(\left|x^U+x^L-y^U-y^L\right| - \sqrt{2}\,(x^U-x^L)\right)_+^2\Bigg] \\ & - \frac{1}{2}\Bigg[(x^U-x^L)\left|y^U+y^L\right| + (y^U-y^L)\left|x^U+x^L\right| \\ & \quad + (x^U-x^L)(y^U-y^L) \\ & \quad - \min\Big\{(x^U-x^L)\left|y^U+y^L\right|,\ (y^U-y^L)\left|x^U+x^L\right|, \\ & \qquad\qquad (x^U-x^L)(y^U-y^L)\Big\}\Bigg],\end{aligned}} \tag{5.22}$$

where $(q)_+ := \max\{q, 0\}$.

Thus,

$$\begin{aligned}\Gamma < 0 &\iff \Delta_{\text{rot}} < \Delta_{\text{orig}}, \\ \Gamma = 0 &\iff \Delta_{\text{rot}} = \Delta_{\text{orig}}, \\ \Gamma > 0 &\iff \Delta_{\text{rot}} > \Delta_{\text{orig}}.\end{aligned} \tag{5.23}$$

The expression (5.20) is an exact necessary-and-sufficient comparison criterion. It also shows that the comparison depends jointly on the dimensions of the rectangle and its position relative to the coordinate axes. The inequality $x_{hr} > y_{hr}$ affects the relative widths $\beta > \alpha$, but does not determine the sign of Γ.

PROPOSITION 5.3 (Absence of universal range dominance). *The condition*

$$x_{hr} > y_{hr}$$

does not imply a fixed ordering between Δ_{rot} *and* Δ_{orig}*. Under this condition, each of the relations*

$$\Delta_{\text{rot}} < \Delta_{\text{orig}}, \qquad \Delta_{\text{rot}} = \Delta_{\text{orig}}, \qquad \Delta_{\text{rot}} > \Delta_{\text{orig}}$$

can occur.

Proof. Consider rectangles centered at the origin, so that

$$h = k = 0.$$

Then

$$S = D = P = Q = 0.$$

Equations (5.6) and (5.16) reduce to

$$\Delta_{\text{rot}} = \frac{x_{hr}^2 + y_{hr}^2}{2}, \qquad \Delta_{\text{orig}} = 2x_{hr}y_{hr}. \tag{5.24}$$

Let

$$\rho := \frac{x_{hr}}{y_{hr}} > 1.$$

Then

$$\Gamma = \frac{y_{hr}^2}{2}\left(\rho^2 - 4\rho + 1\right). \tag{5.25}$$

For example,

$$\rho = 2 \quad \Longrightarrow \quad \Gamma < 0,$$

whereas

$$\rho = 2 + \sqrt{3} \quad \Longrightarrow \quad \Gamma = 0,$$

and

$$\rho = 4 \quad \Longrightarrow \quad \Gamma > 0.$$

All three choices satisfy $\rho > 1$, completing the proof. ∎

5.4. Centered rectangles. The preceding proof yields a complete characterization for rectangles centered at the origin.

THEOREM 5.4. *Suppose*

$$h = k = 0 \qquad \textit{and} \qquad x_{hr} > y_{hr} > 0.$$

Then

$$\Delta_{\text{rot}} = \frac{x_{hr}^2 + y_{hr}^2}{2}, \qquad \Delta_{\text{orig}} = 2x_{hr}y_{hr}. \tag{5.26}$$

Moreover,

$$\Delta_{\text{rot}} \begin{cases} < \Delta_{\text{orig}}, & 1 < \dfrac{x_{hr}}{y_{hr}} < 2 + \sqrt{3}, \\ = \Delta_{\text{orig}}, & \dfrac{x_{hr}}{y_{hr}} = 2 + \sqrt{3}, \\ > \Delta_{\text{orig}}, & \dfrac{x_{hr}}{y_{hr}} > 2 + \sqrt{3}. \end{cases} \tag{5.27}$$

Proof. From (5.24),

$$\Delta_{\text{rot}} - \Delta_{\text{orig}} = \frac{1}{2}\left(x_{hr}^2 - 4x_{hr}y_{hr} + y_{hr}^2\right).$$

Dividing by $y_{hr}^2/2 > 0$ gives

$$\rho^2 - 4\rho + 1, \qquad \rho := \frac{x_{hr}}{y_{hr}}.$$

The roots are

$$\rho = 2 - \sqrt{3} \qquad \text{and} \qquad \rho = 2 + \sqrt{3}.$$

Because $\rho > 1$, only the second root is relevant. The sign classification in (5.27) follows from the positive leading coefficient of the quadratic. ∎

Theorem 5.4 shows that, for a rectangle centered at the origin, rotation reduces the bilinear range when $1 < x_{hr}/y_{hr} < 2+\sqrt{3}$, the two ranges coincide when $x_{hr}/y_{hr} = 2 + \sqrt{3}$, and rotation increases the bilinear range when $x_{hr}/y_{hr} > 2 + \sqrt{3}$.

5.5. Geometric interpretation. The distinction between Δ_{orig} and Δ_{rot} follows from the orientation of the feasible boundaries relative to the bilinear surface.

On the original rectangle, each edge fixes one variable. The restriction of xy to any edge is therefore affine, and its extrema occur at the endpoints of that edge. Hence, all extrema over $\mathcal{R}_{\text{orig}}$ occur at vertices.

On the rotated region, the edges have the forms

$$x' + y' = a_i \qquad \text{or} \qquad x' - y' = b_j.$$

Along $x' + y' = a_i$,

$$x'y' = a_i x' - (x')^2,$$

which is strictly concave and may attain its maximum in the relative interior of the edge. Along $x' - y' = b_j$,

$$x'y' = (x')^2 - b_j x',$$

which is strictly convex and may attain its minimum in the relative interior of the edge.

Accordingly, the range over the rotated region depends not only on the four vertex values but also on whether the intervals $[a_1, a_2]$ and $[b_1, b_2]$ contain the origin. These conditions are governed by

$$|h + k| \le \sqrt{2}\, y_{hr}$$

and

$$|h - k| \le \sqrt{2}\, x_{hr},$$

respectively.

Finally, the assumption

$$x_U - x_L > y_U - y_L$$

implies only that the feasible interval for $x' - y'$ is wider than the feasible interval for $x' + y'$. It does not control the locations of these intervals relative to the origin and therefore cannot, by itself, establish that one bilinear range dominates the other.

6. Conclusions and Future Work. In this work, we investigated the impact of introducing 45°-oblique cuts within the spatial branch-and-bound (sBB) framework, as opposed to the standard practice of using parallel axis cuts. We analyzed the geometry of the resulting partitions and derived directionally tighter relaxations for the corresponding sub-regions, demonstrating that these relaxations can improve upon the classical McCormick envelopes. In addition, we provided closed-form expressions that quantify the improvement in the relaxation bounds relative to the McCormick bounds.

A key limitation of this approach, however, is that oblique cuts may generate sub-regions with geometries more complex than the diamond-shaped regions studied in this work. In particular, such cuts can lead to triangular or trapezoidal regions, for which deriving tight and computationally efficient relaxations may be more challenging.

Overall, this work serves as an initial step toward understanding branching strategies based on oblique partitioning. Future research directions include deriving effective relaxations for the triangular and trapezoidal sub-regions that may arise from oblique partitioning, developing implementable oblique branching rules, and integrating these ideas into a full spatial branch-and-bound framework to evaluate their effects on relaxation quality, node counts, and computational time.

Acknowledgments. The authors would like to thank Dr. Victoria C.P Chen for her guidance, the Center on Stochastic Modeling, Optimization and Statistics (COSMOS) at the University of Texas at Arlington and National Science Foundation (NSF-CHE-2108767) for partially funding this research.

REFERENCES

[1] N. Adhya, M. Tawarmalani, and N. V. Sahinidis, *A lagrangian relaxation approach for the pooling problem*, Industrial & Engineering Chemistry Research, 38 (1999), pp. 1956–1972, https://doi.org/10.1021/ie980691p, https://doi.org/10.1021/ie980691p.

[2] C. S. Adjiman, S. Dallwig, C. A. Floudas, and A. Neumaier, *A global optimization method, αBB, for general twice-differentiable constrained NLPs — i. theoretical advances*, Computers & Chemical Engineering, 22 (1998), pp. 1137–1158, https://doi.org/10.1016/S0098-1354(98)00027-1, https://doi.org/10.1016/S0098-1354(98)00027-1.

[3] C. S. Adjiman, S. Dallwig, C. A. Floudas, and A. Neumaier, *A global optimization method, αBB, for general twice-differentiable constrained NLPs — ii. computational results*, Computers & Chemical Engineering, 22 (1998), pp. 1159–1179, https://doi.org/10.1016/S0098-1354(98)00028-3, https://doi.org/10.1016/S0098-1354(98)00028-3.

[4] F. A. Al-Khayyal and J. E. Falk, *Jointly constrained biconvex programming*, Mathematics of Operations Research, 8 (1983), pp. 273–286, https://doi.org/10.1287/moor.8.2.273, https://doi.org/10.1287/moor.8.2.273.

[5] C. Audet, J. Brimberg, P. Hansen, S. L. Digabel, and N. Mladenović, *Pooling problem: Alternate formulations and solution methods*, Management Science, 50 (2004), pp. 761–776, https://doi.org/10.1287/mnsc.1030.0207, https://doi.org/10.1287/mnsc.1030.0207.

[6] P. Belotti, C. Kirches, S. Leyffer, J. Linderoth, J. Luedtke, and A. Mahajan, *Mixed-integer nonlinear optimization*, Acta Numerica, 22 (2013), p. 1–131, https://doi.org/10.1017/S0962492913000032.

[7] P. Belotti, J. Lee, L. Liberti, F. Margot, and A. Wächter, *Branching and bounds tightening techniques for non-convex minlp*, Optimization Methods and Software, 24 (2009), pp. 597–634, https://doi.org/10.1080/10556780903087124.

[8] K. Bestuzheva, A. Gleixner, and T. Achterberg, *Efficient separation of rlt cuts for implicit and explicit bilinear products*, in Integer Programming and Combinatorial Optimization, A. Del Pia and V. Kaibel, eds., Cham, 2023, Springer International Publishing, pp. 14–28.

[9] C. Buchheim and A. Wiegele, *Semidefinite relaxations for non-convex quadratic mixed-integer programming*, Mathematical Programming, 141 (2013), pp. 1–18, https://doi.org/10.1007/s10107-012-0534-y, https://doi.org/10.1007/s10107-012-0534-y.

[10] S. Burer and A. N. Letchford, *Non-convex mixed-integer nonlinear programming: A survey*, Surveys in Operations Research and Management Science, 17 (2012), pp. 97–106, https://doi.org/10.1016/j.sorms.2012.08.001, https://doi.org/10.1016/j.sorms.2012.08.001.

[11] C. Coffrin, H. L. Hijazi, and P. V. Hentenryck, *Strengthening convex relaxations with bound tightening for power network optimization*, in Principles and Practice of Constraint Programming (CP 2015), G. Pesant, ed., vol. 9255 of Lecture Notes in Computer Science, Cham, 2015, Springer, pp. 39–57, https://doi.org/10.1007/978-3-319-23219-5_4, https://doi.org/10.1007/978-3-319-23219-5_4.

[12] S. S. Dey and A. Gupte, *Analysis of MILP techniques for the pooling problem*, Operations Research, 63 (2015), pp. 412–427, https://doi.org/10.1287/opre.2015.1357, https://doi.org/10.1287/opre.2015.1357.

[13] T. Fujie and M. Kojima, *Semidefinite programming relaxation for nonconvex quadratic programs*, Journal of Global Optimization, 10 (1997), pp. 367–380, https://doi.org/10.1023/A:1008200424561, https://doi.org/10.1023/A:1008200424561.

[14] Q. Gemine, D. Ernst, Q. Louveaux, and B. Cornélusse, *Relaxations for multi-period optimal power flow problems with discrete decision variables*, in 2014 Power Systems Computation Conference, 2014, pp. 1–7, https://doi.org/10.1109/PSCC.2014.7038396.

[15] A. Gupte, S. Ahmed, S. S. Dey, et al., *Relaxations and discretizations for the pooling problem*, Journal of Global Optimization, 67 (2017), pp. 631–669, https://doi.org/10.1007/s10898-016-0434-4, https://doi.org/10.1007/s10898-016-0434-4.

[16] I. Harjunkoski, R. Pörn, and T. Westerlund, *Exploring the convex transformations for solving non-convex bilinear integer problems*, Computers & Chemical Engineering, 23 (1999), pp. S471–S474, https://doi.org/10.1016/S0098-1354(99)80119-8, https://doi.org/10.1016/S0098-1354(99)80119-8.

[17] I. Harjunkoski, R. Pörn, T. Westerlund, and H. Skrifvars, *Different strategies for solving bilinear integer non-linear programming problems with convex transformations*, Computers & Chemical Engineering, 21 (1997), pp. S487–S492, https://doi.org/10.1016/S0098-1354(97)87592-5, https://doi.org/10.1016/S0098-1354(97)87592-5.

[18] T. He and M. Tawarmalani, *A new framework to relax composite functions in nonlinear programs*, Mathematical Programming, 190 (2021), pp. 427–466, https://doi.org/10.1007/s10107-020-01541-x, https://doi.org/10.1007/s10107-020-01541-x.

[19] C. Helmberg, F. Rendl, and R. Weismantel, *A semidefinite programming approach to the quadratic knapsack problem*, Journal of Combinatorial Optimization, 4 (2002), pp. 197–215, https://doi.org/10.1023/A:1020512223945, https://doi.org/10.1023/A:1020512223945.

[20] H. Konno and M. Inori, *Bond portfolio optimization by bilinear fractional programming*, Journal of the Operations Research Society of Japan, 32 (1989), pp. 143–158, https://doi.org/10.15807/jorsj.32.143.

[21] J. Luedtke, M. Namazifar, and J. Linderoth, *Some results on the strength of relaxations of multilinear functions*, Mathematical Programming, Series B, 136 (2012), pp. 325–351, https://doi.org/10.1007/s10107-012-0606-z, https://doi.org/10.1007/s10107-012-0606-z.

[22] G. P. McCormick, *Computability of global solutions to factorable nonconvex programs: Part i — convex underestimating problems*, Mathematical Programming, 10 (1976), pp. 147–175, https://doi.org/10.1007/BF01580665, https://doi.org/10.1007/BF01580665.

[23] R. Misener and C. A. Floudas, *Antigone: Algorithms for continuous / integer global optimization of nonlinear equations*, J. of Global Optimization, 59 (2014), p. 503–526, https://doi.org/10.1007/s10898-014-0166-2, https://doi.org/10.1007/s10898-014-0166-2.

[24] A. D. Rikun, *A convex envelope formula for multilinear functions*, Journal of Global Optimization, 10 (1997), pp. 425–437, https://doi.org/10.1023/A:100828683, https://doi.org/10.1023/A:100828683.

[25] H. S. Ryoo and N. V. Sahinidis, *Global optimization of nonconvex nlps and minlps with applications in process design*, Computers & Chemical Engineering, 19 (1995), pp. 551–566, https://doi.org/10.1016/0098-1354(94)00097-2, https://doi.org/10.1016/0098-1354(94)00097-2.

[26] N. V. Sahinidis, *Baron: A general purpose global optimization software package*, Journal of Global Optimization, 8 (1996), pp. 201–205, https://api.semanticscholar.org/CorpusID:206770254.

[27] A. M. Schweidtmann, D. Bongartz, D. Grothe, T. Kerkenhoff, X. Lin, J. Najman, and A. Mitsos, *Deterministic global optimization with gaussian processes embedded*, Mathematical Programming Computation, 13 (2021), pp. 553–581, https://doi.org/10.1007/s12532-021-00204-y, https://doi.org/10.1007/s12532-021-00204-y.

[28] J. K. Scott, M. D. Stuber, and P. I. Barton, *Generalized McCormick relaxations*, Journal of Global Optimization, 51 (2011), pp. 569–606, https://doi.org/10.1007/s10898-011-9664-7,

https://doi.org/10.1007/s10898-011-9664-7.

[29] H. D. Sherali and A. Alameddine, *A new reformulation-linearization technique for bilinear programming problems*, Journal of Global Optimization, 2 (1992), pp. 379–410, https://doi.org/10.1007/BF00122429, https://doi.org/10.1007/BF00122429.

[30] E. M. B. Smith and C. C. Pantelides, *A symbolic reformulation/spatial branch-and-bound algorithm for the global optimisation of nonconvex minlps*, Computers & Chemical Engineering, 23 (1999), pp. 457–478, https://api.semanticscholar.org/CorpusID:122302749.

[31] M. Tawarmalani and N. V. Sahinidis, *Convexification and Global Optimization in Continuous and Mixed-Integer Nonlinear Programming: Theory, Algorithms, Software, and Applications*, Kluwer Academic Publishers, Dordrecht, The Netherlands, 2002, https://doi.org/10.1007/978-1-4757-5047-8, https://doi.org/10.1007/978-1-4757-5047-8.

[32] M. Tawarmalani and N. V. Sahinidis, *Global optimization of mixed-integer nonlinear programs: A theoretical and computational study*, Mathematical Programming, 99 (2004), pp. 563–591, https://doi.org/10.1007/s10107-003-0467-6, https://doi.org/10.1007/s10107-003-0467-6.

[33] M. Tawarmalani and N. V. Sahinidis, *A polyhedral branch-and-cut approach to global optimization*, Mathematical Programming, 103 (2005), pp. 225–249, https://doi.org/10.1007/s10107-005-0582-8, https://doi.org/10.1007/s10107-005-0582-8.

[34] A. Tsoukalas and A. Mitsos, *Multivariate McCormick relaxations*, Journal of Global Optimization, 59 (2014), pp. 633–662, https://doi.org/10.1007/s10898-014-0176-0, https://doi.org/10.1007/s10898-014-0176-0. Received: 17 April 2013 / Accepted: 18 March 2014 / Published online: 2 April 2014.

[35] M. E. Wilhelm and M. D. Stuber, *Improved convex and concave relaxations of composite bilinear forms*, Journal of Optimization Theory and Applications, 197 (2023), pp. 174–204, https://doi.org/10.1007/s10957-023-02196-2, https://doi.org/10.1007/s10957-023-02196-2.